ARCHIVES OF TRANSPORT *ISSN (print):* *0866-9546*
Volume 49, Issue 1, 2019 ***e-ISSN (online):*** *2300-8830*
DOI: *10.5604/01.3001.0013.2775*

DRIVING ENERGY MANAGEMENT OF FRONT-AND-REAR-MOTOR-DRIVE ELECTRIC VEHICLE BASED ON HYBRID RADIAL BASIS FUNCTION

Binbin SUN[1], Tiezhu ZHANG[2], Wenqing GE[3], Cao TAN[4], Song GAO[5]

[1, 2, 3, 4, 5] *Shandong University of Technology, School of Transportation and Vehicle Engineering, Zibo, Shandong, China*

Abstract:

This paper presents mathematical methods to develop a high-efficiency and real-time driving energy management for a front-and-rear-motor-drive electric vehicle (FRMDEV), which is equipped with an induction motor (IM) and a permanent magnet synchronous motor (PMSM). First of all, in order to develop motor-loss models for energy optimization, database of with three factors, which are speed, torque and temperature, was created to characterize motor operation based on HALTON sequence method. The response surface model of motor loss, as the function of the motor-operation database, was developed with the use of Gauss radial basis function (RBF). The accuracy of the motor-loss model was verified according to statistical analysis. Then, in order to create a two-factor energy management strategy, the modification models of the torque required by driver (Td) and the torque distribution coefficient (β) were constructed based on the state of charge (SOC) of battery and the motor temperature, respectively. According to the motor-loss models, the fitness function for optimization was designed, where the influence of the non-work on system consumption was analyzed and calculated. The optimal β was confirmed with the use of the off-line particle swarm optimization (PSO). Moreover, to achieve both high accuracy and real-time performance under random vehicle operation, the predictive model of the optimal β was developed based on the hybrid RBF. The modeling and predictive accuracies of the predictive model were analyzed and verified. Finally, a hardware-in-loop (HIL) test platform was developed and the predictive model was tested. Test results show that, the developed predictive model of β based on hybrid RBF can achieve both real-time and economic performances, which is applicable to engineering application. More importantly, in comparison with the original torque distribution based on rule algorithm, the torque distribution based on hybrid RBF is able to reduce driving energy consumption by 9.51% under urban cycle.

Keywords: *front-and-rear-motor-drive electric vehicle, energy management, real-time torque distribution, energy optimization, fitness function, hybrid radial basis function, predictive model, hardware-in-loop test*

To cite this article:

Sun, B., Zhang, T., Ge, W., Tan, C., Gao, S., 2019. Driving energy management of front-and-rear-motor-drive electric vehicle based on hybrid radial basis function. Archives of Transport, 49(1), 47-58. DOI: https://doi.org/10.5604/01.3001.0013.2775

Contact:
1) sunbin_sdut@126.com[https://orcid.org/0000-0003-2310-8869], 2) [https://orcid.org/0000-0001-6692-5207],
3) [https://orcid.org/0000-0002-1060-273X], 4) [https://orcid.org/0000-0002-0863-0010], 5) gaos546@126.com [https://orcid.org/0000-0002-3367-2546] - corresponding author

1. Introduction

Development of high-performance electric vehicles (EVs) has been proved as an effective way to relieve the challenges of fossil energy crisis and environmental pollution (Merkisz-Guranowska, et al., 2014, China Automotive Technology Research Center, et al., 2015, Shawn A. Adderly, et al., 2018). Owing to the advantages of high dynamic property, stability and safety, FRMDEV has attracted a lot of attention (Binbin Sun, et al. 2018). Currently, based on FRMDEV, researches focusing on the controls of regenerative brake, driving stability and failure safety have been conducted, and remarkable achievements have been achieved (Sun Daxu, et al., 2016, Binbin Sun, et al., 2016, Guo H., et al., 2014, Nobuyoshi Mutoh, 2012). Torque distribution between front and rear motors, aiming at energy efficiency optimization, has a fundamental impact on the driving economy of FRMDEV, but is still lack of study (M. Satyendra Kumar, 2017).

Currently, in order to achieve real-time torque distribution of vehicle with dual or multiple power sources, rule algorithm is the most commonly used method (Abdul Rauf Bhatti, et al., 2018, Jiankun Peng, 2017). However, this kind of algorithm is still unable to achieve the optimal energy efficiency (Yin Shi, 2014). Theoretically, torque distribution strategy based on optimal algorithm can achieve highest-efficiency drive of vehicle, but the real-time performance based on this method is still difficult to be guaranteed for engineering application (Syuan-Yi Chen, et al., 2018, N. Sulaiman, et al., 2018, Zhang Xi, 2013).

Consequently, in this paper, based on hybrid RBF, a predictive torque distribution model that can balance both energy efficiency optimization and real-time property was developed. Firstly, a high-precision model of motor power loss based on Gauss RBF was developed to calculate the fitness value of the torque distribution optimization model. Then, a fitness function model dealing with the drag loss of non-work motor was designed, and the off-line database of the optimal β was created based on PSO. Furthermore, a predictive model of torque distribution with the form of polynomial and Gauss RBF was established and analyzed. Finally, a new torque distribution model for FRMDEV with induction motor (IM) and permanent magnet synchronous motor (PMSM) was verified with the use of HIL method.

2. Configuration of FRMDEV

Figure 1 shows the powertrain system of the currently developed FRMDEV. The power system mainly consists of the battery system, the front and rear power-train systems. In order to take the economic advantages of different types of motors (Binbin Sun, et al., 2017), the front and rear axles are equipped with a PMSM and an IM, respectively. Transmissions with different one-speed ratios are used in the front and rear axle transmission systems. By the CAN bus, the vehicle control unit (VCU) communicates with the front and rear motor control units (MCUs) and the battery management systems (BMS). Moreover, based on the monitored statuses of vehicle and key components, the VCU run the torque distribution model to achive the single-motor-drive or dual-motor-drive mode (SMDM or DMDM). Some remarks about the PMSM and IM were designed in our previous research. The connection between the parameters of motor and the characteristics of FRMDEV was also confirmed and verified (Sun B., et al., 2016).

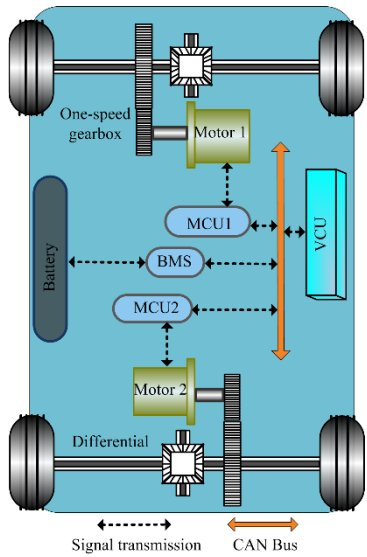

Fig. 1. Power systems of FRMDEV

3. Development of motor-loss model

High-precise model of motor power loss is the key to torque distribution optimization of FRMDEV, which is mainly affected by operating conditions (speed, torque and temperature). If set the operating

conditions and the power loss as the inputs and output of motor power loss function, how to construct the high-precise dominant function relationship between them, is the key problem to be solved in this section.

3.1. Response surface model of power loss

For motor power loss model with uncertain function relation between the input factors and output response, the size, randomness and uniformity of operating sample should be dealt with. Consequently, in this paper, as shown in table 1, a three-factor sample database with the size of 250 to characterize motor operations is developed based on the HALTON sequence method. Furthermore, based on the developed dual-motor test platform shown in figure 2, the motor power losses under the designed samples are tested to create the response database. Temperature parameters of the IM and PMSM are provided by the manufacturers. They are obtained by CAN communication between MCU and VCU.

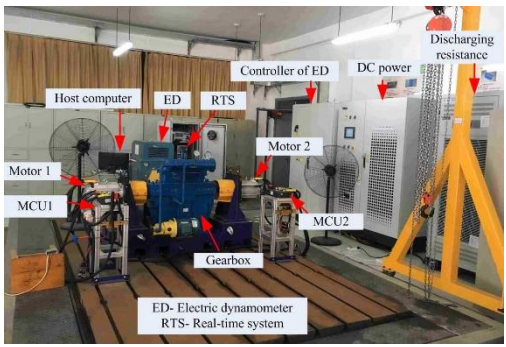

Fig. 2. Dual-motor test platform

Referring to the input and response databases shown in table 1, to achieve high-accuracy dominant function relationship between the two databases, the Gauss RBF and stepwise regression analysis theory are adopted to create the response surface model of the IM power loss as shown in formula 1.

$$\begin{cases} \hat{P}_{ls} = \sum_{i=1}^{m} \phi_{i\_dl} w_i + \zeta \\ \phi_{i\_dl} = \exp\left(-\dfrac{\left\| \overrightarrow{x_{dl}} - \overrightarrow{C_{i\_dl}} \right\|^2}{2b_i^2} \right) \end{cases} \tag{1}$$

Where dl represents dimensionless form, $\hat{P}_{ls}$ is the predictive motor power loss, w_i is weight coefficient, ϕ_{i_dl} is Gauss basis function, $\overrightarrow{x_{dl}}$ is the input vector of RBF defined as $[n_{\_dl}, T_{\_dl}, t_{em\_dl}]^T$, $\overrightarrow{C_{i\_dl}}$ is central vector of i^{th} network nodes as shown in formula 2, b_i is base width, ζ is regularization parameter.

$$\overrightarrow{C_{i\_dl}} = \begin{bmatrix} n_{i\_dl} = (L_{max} - L_{min}) \dfrac{n_i - n_{min}}{n_{max} - n_{min}} + L_{min} \\ T_{i\_dl} = (L_{max} - L_{min}) \dfrac{T_i - T_{min}}{T_{max} - T_{min}} + L_{min} \\ t_{em\_i\_dl} = (L_{max} - L_{min}) \dfrac{t_{em\_i} - t_{em\_min}}{t_{em\_max} - t_{em\_min}} + L_{min} \end{bmatrix} \tag{2}$$

Where n_{i_dl}, T_{i_dl} and $t_{em\_i\_dl}$ represent the dimensionless speed, torque and temperature, n_{min} and n_{max} are the maximum and minimum speeds, T_{em_max} and T_{em_min} are the maximum and minimum torques, t_{em_max} and t_{em_min} are the maximum and minimum temperatures, L_{min} and L_{max} represent the minimum and maximum dimensionless numbers.

Table 1. Input factors and responses of power loss

	Input factors			Responses
Num.	Speed/r.min^{-1}	Torque/N.m	Tem. /°C	Power loss/W
1	550	66	65	2780.17
2	2350	36	45	3341.51
3	1300	62	45	3466.86
…	…	…	…	…
248	1600	35	65	2587.25
249	500	58	55	2137.68
250	4000	35	70	4870.45

The key parameters of the model are presented in table 2, where Num. and Tem. are short for Number and Temperature respectively. Moreover, the response surface model of PMSM power loss can also be created with the use of this mathematical method.

3.2. Verification of model accuracy

Taking the power loss model of IM for example, the R^2 and RMSE of the model are confirmed as 0.997 and 131.972, which means that the modeling accuracy of this model based on Guass RBF is high.

Table 2. Key parameters of IM power loss based on Gauss RBF

Num.	w_i ($\times 10^3$)	RBF centers (dimensionless form)		
		n_{i_dl}	T_{i_dl}	$t_{em\_i\_dl}$
1	10.634	-0.91111	-0.75060	-0.2
2	10.739	0.15556	-0.79652	0.3
3	-8.670	-0.24444	-0.12208	0.3
…	…	…	…	…
9	3.008	0.64444	-0.881	0.3
10	5.962	0.22222	-0.03264	-0.2
11	-8.943	-0.64444	-0.42016	0

Furthermore, as the studentized residuals of the model shown in figure 3, most of the studentized residuals are within [-2, +2], which further indicates that response surface model of IM power loss is with high accurancy. Furthermore, the modeling accuracy of PMSM power loss model can also be verified in the same way.

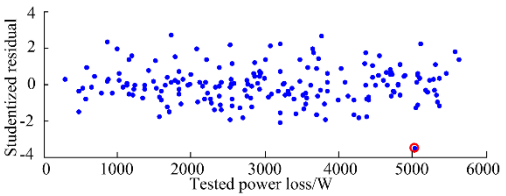

Fig. 3. Studentized residuals of IM power loss model

To verify the prdictive accuracy of the response surface model developed for IM power loss, as show in table 3, an additional sample of IM operations with 50 capacity is designed randomly based on the Halton sequence method. In the table, N is the number of operations, P_t and P_p are the tested and predictive power losses, R_e is the relative error.

For the new operating database, the tested and calculated power losses can be confirmed based on the dual-motor test platform and the Guass-RBF power loss model. The tested and calculated results show that, most of the differences between the tested and calculated values are small than 4%, which means that the response surface model based on Guass RBF has high-prediction accuracy. Furthermore, the predictive accuracy of PMSM power loss model can also be verified in the same way.

Table 3. Verification result of predictive accuracy

	New samples			Predictive accuracy		
Num.	n/r.min^{-1}	T/N.m	t_{em}/°C	P_t/W	P_p/W	R_e/%
1	1400	30	55	1991.67	1925.24	3.45
2	1000	50	65	2664.73	2593.16	2.76
3	1950	20	45	1847.49	1896.61	2.59
			…			
48	550	55	60	2032.63	2130.86	4.61
49	2600	60	50	5771.62	5600.25	3.06
50	3150	20	65	3447.96	3308.35	4.22

4. Predictive model of torque distribution

As shown in figure 3, method for modeling multi-objective strategy of brake force distribution is designed. First of all, based on HALTON sequence method, an input database characterizing FRMDEV operation is constructed, which is defined as the factor database. Then, for any given brake condition of the factor database, a output database consisting of multi-objective brake force distribution is optimized, with the use of off-line PSO, which is defined as the response database. Finally, based on hybrid RBF, the dominant function relationship between the factor database and the response database is established.

4.1. Design of vehicle operation database

As shown in figure 4(a), the advantage of the torque distribution model with full-factor operations is that the system model is relatively simple, but on the other hand, the predictive model of torque distribution is much more complex, which will cause negative influences on the real-time performance and accuracy of the predictive model. Consequently, in this paper, a hierarchical control strategy is developed as shown in figure 4(b), where the upper strategy is designed to correct the factor of the torque required by driver (T_d) based on the factor of SOC, the middle layer is the predictive model of torque distribution with two factors (vehicle speed and corrected T_d), the lower layer is developed to correct the output of the predictive model based on the temperature of IM and PMSM (t_{im} and t_{sm}).

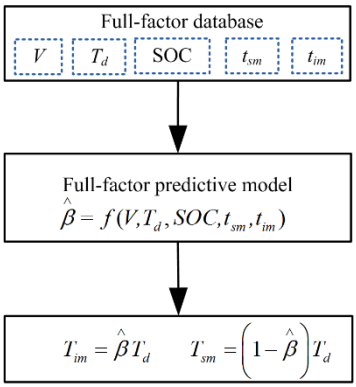

(a) Full-factor torque distribution

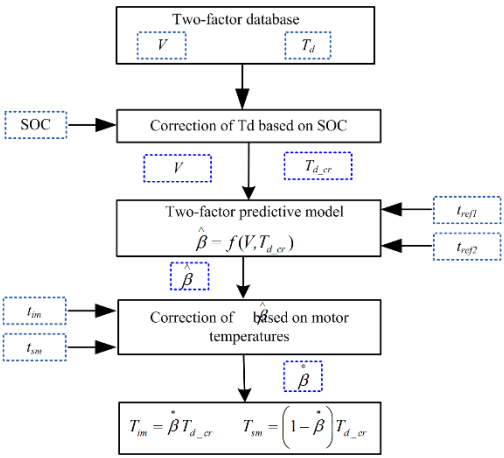

(b) Two-factor torque distribution

Fig. 4. Modeling methods of predictive torque distribution

Given the above analysis, a two-factor database characterizing vehicle operation is designed based on HALTON sequence method. As shown in formula 3, the sample capacity of the random operation database is 600, which can be corrected according to the accuracy of the predictive model.

$$\overrightarrow{X} = \begin{bmatrix} V_1 & T_{d\_1} \\ \vdots & \\ V_k & T_{d\_k} \\ \vdots & \\ V_{600} & T_{d\_600} \end{bmatrix} = \begin{bmatrix} 54.063 & 95.556 \\ \vdots & \\ 8.125 & 106.111 \\ \vdots & \\ 77.188 & 82.222 \end{bmatrix} \tag{3}$$

Where $T_{cha\_max\_soc}$ is the maximum allowed charging torque, which is corrected on the basis of SOC. k_c is a conversion factor of unit, r is the wheel radius, P_{cha_max} is the maximum allowed charging power, f_d is the ratio of the transmission system.

4.2. Correction model of Td based on SOC

As shown in formula 4, the maximum allowable discharge torque of battery is affected by SOC. Specially, when SOC is small, the maximum discharge torque should be limited to prolong the battery life, and if SOC is large, battery is allowed to discharg with high power to ensure vehicle dynamic performance. Furthermore, when SOC is moderate, the maximum allowable discharge torque reduces with the decrease of SOC.

$$T_{dis\_max\_cr} = \begin{cases} T_{dis\_lim} = 0.1 \dfrac{r k_c P_{dis\_max}}{f_d V} & SOC \le 0.3 \\ \dfrac{SOC - 0.2}{0.65} \dfrac{r k_c P_{dis\_max}}{f_d V} & 0.3 < SOC < 0.85 \\ \dfrac{r k_c P_{dis\_max}}{f_d V} & SOC \ge 0.85 \end{cases} \tag{4}$$

Where $T_{dis\_max\_cr}$ is the corrected maximum allowable discharge torque of battery, T_{dis_lim} is the limited discharge torque, k_c is unit conversion factor, r is the radius of wheel, P_{dis_max} is maximum allowable discharge power of battery, f_d is the ratio of transmission system.

Taking the maximum allowable discharge torque of battery and the peak torque of motors, the correction model of T_d can be expressed as follow:

$$T_{d\_cr} = \min\left(T_d, T_{dis\_max\_cr}, T_{im\_max} + T_{sm\_max}\right) \tag{5}$$

4.3. Correction model of predictive β

Here, assume that the reference temperatures of PMSM and IM are t_{ref1} and t_{ref2} respectively, the optimal torque distribution coefficient based on the two-factor predictive model is $\hat{\beta}_o$, which means when β is $\hat{\beta}_o$, the theoretical loss of the dual-motor system is minimal. According to the control modes of PMSM and IM, it can be derived that:

$$\begin{cases} P_{co}\left(\hat{\beta}_o\right)=\left[\left(1-\hat{\beta}_o\right)I\right]^2 R_{ref1}+\left(\hat{\beta}_o I-I_{d2}\right)^2 R_{ref2\_ro} \\ \quad +{I_{d2}}^2 R_{ref2\_st} \\ \left.\dfrac{\partial P_{co}(\beta)}{\partial\beta}\right|_{\beta=\hat{\beta}_o}=0 \end{cases} \tag{6}$$

Where R_{ref1} is the armature resistance of PMSM under the given reference temperature of t_{ref1}, R_{ref2_ro} and R_{ref2_st} are the winding resistances of IM rotor and stator under the given reference temperature of t_{ref2}, I is the system current, I_{d2} is excitation current of IM, P_{co} is the copper loss of the dual-motor system.

Referring to the formula discussed above, it can be further derived that:

$$I_d I R_{ref2\_ro}=\hat{\beta}_o R_{ref2\_ro}+\left(1-\hat{\beta}_o\right)I^2 R_{ref1} \tag{7}$$

Actually, the temperatures of the dual motors are different from the reference temperatures. Consequently, the copper loss of the dual-motor system dealing with the correction of motor temperature can be derived as:

$$\begin{aligned} P_{co}(\beta)=&\left[(1-\beta)I\right]^2 k_1 R_{ref1}+{I_{d2}}^2 k_3 R_{ref2\_st} \\ &+\left(\beta I-I_{d2}\right)^2 k_2 R_{ref2\_ro} \end{aligned} \tag{8}$$

Where k_1, k_2 and k_3 are the ratios of the actual resistances to the referential ones.

Furthermore, for actual working condition, it is assumed that the copper loss of the dual-motor system is minimal when β is= $\overset{*}{\beta}_o$, which means:

$$\begin{cases} \left.\dfrac{\partial P_{co}(\beta)}{\partial\beta}\right|_{\beta=\overset{*}{\beta}_o}=0 \\ \overset{*}{\beta}_o=\dfrac{k_1 I^2 R_{ref1}+k_2 I_d I R_{ref2\_ro}}{k_1 I^2 R_{ref1}+k_2 I^2 R_{ref2\_ro}} \end{cases} \tag{9}$$

Where $\overset{*}{\beta}_o$ is the optimal torque distribution coefficient based on the correction of motor temperature.

Given the above analysis, the correction model of $\hat{\beta}_o$ can be derived as:

$$\overset{*}{\beta}_o=\frac{k_1 R_{ref1}+k_2\left[\hat{\beta}_o R_{ref2\_ro}+\left(1-\hat{\beta}_o\right)R_{ref1}\right]}{k_1 R_{ref1}+k_2 R_{ref2\_ro}} \tag{10}$$

4.4. Design of fitness function

Taking the i^{th} sample point of vehicle operations for example (V_i, T_{di}), the optimization model of β under this operation can be established as follows.

Find: $\beta=\dfrac{T_{im}}{T_{d\_cr}}$

Min:

$$f(\beta)=\frac{\psi_{im}\beta T_{d\_cr} f_{im\_d} V}{\eta_{im}\eta_{b\_dis}\eta_{T\_im} k_c r}+\frac{\psi_{sm}(1-\beta)T_{d\_cr} f_{sm\_d} V}{\eta_{sm}\eta_{b\_dis}\eta_{T\_sm} k_c r}$$

Satisfy: $\beta_{max} T_{d\_cr}\le T_{im\_max}$

$$\begin{aligned} &(1-\beta_{min})T_{d\_cr}\le T_{sm\_max} \\ &0\le\beta\le 1 \\ &f_{sm\_d}V/rk_c\le n_{sm\_max} \\ &f_{im\_d}V/rk_c\le n_{im\_max} \end{aligned} \tag{11}$$

Where the $f(\beta)$ is the fitness function of β, η_{im} and η_{sm} are the efficiencies of IM and PMSM, which can be confirmed according to the power-loss models developed above, η_{b_dis} is the discharge efficiency of battery, η_{T_im} and η_{T_sm} represent the mechanical efficiency of IM and PMSM, ψ_{im} and ψ_{sm} are the penalty functions of IM and PMSM to prevent single IM or PMSM from overloading for a long time, which are modeled as follows.

$$\begin{cases} \psi_{im}=1 & \beta T_{d\_cr}\le 1.25T_{im\_e} \\ \psi_{im}=\dfrac{\beta T_{d\_cr}}{T_{im\_e}\eta_{T\_im}} & \beta T_{d\_cr}>1.25T_{im\_e} \end{cases} \tag{12}$$

$$\begin{cases} \psi_{sm}=1 & (1-\beta)T_{d\_cr}\le T_{sm\_e} \\ \psi_{sm}=\dfrac{(1-\beta)T_{d\_cr}}{T_{sm\_e}\eta_{T\_sm}} & (1-\beta)T_{d\_cr}>T_{sm\_e} \end{cases} \tag{13}$$

Where T_{im_e} and T_{sm_e} are the nominal torques of IM and PMSM.

Furthermore, when FRMDEV operates under SMDM, the non-work motor is motored, which actually causes drag loss. Consequently, $f(\beta)$ discussed above should be modified based on the drag loss of the non-work motor. Specially,

(1) If β is within (0, 1), as there is no non-work motor drag loss, $f(\beta)$ is:

$$f(\beta)_{\_cr} = f(\beta) \tag{14}$$

(2) If β is 0, non-work IM is motored by vehicle, $f(\beta)$ is modified as:

$$f(\beta)_{\_cr} = f(\beta) + P_{im\_mt} \tag{15}$$

(3) If β is 1, non-work PMSM is motored by vehicle, $f(\beta)$ is modified as:

$$f(\beta)_{\_cr} = f(\beta) + P_{sm\_mt} \tag{16}$$

Where $f(\beta)_{\_cr}$ is the modified fitness function that takes the drag loss of non-work motor into account, P_{im_mt} and P_{sm_mt} represent the drag losses caused by IM and PMSM respectively.

4.5. Offline optimization based on PSO

PSO is used to optimize β for the two-factor operation database. Specially, the program of the off-line PSO is as follows. Firstly, the particle swarm is randomly generated according to the accessible flight range, which consists of the random β_1, β_2…β_n with different initial velocities. Secondly, in each iteration step, for any particle (β_i), the fitness value of it can be calculated according to the fitness functions discussed above. Then, according to the memory ability of PSO, for any particle (β_i), its fitness value is compared with the best one it has experienced and the best one the particle swarm has experienced, which is used to update the velocity and direction of β_i. Repeating the iteration steps discussed above, the optimal β_i can be achieved finally.

As shown in figure 5, taking the operating condition V=25.78km.h^{-1}, T_d=16.48N.m for example, under this operation, the optimal β aiming at the minimum power loss converges to 0, and the fitness value converges to 690.86W.

According to the off-line optimization program discussed above, the optimal response database for the two-factor vehicle operation database is created as shown in formula 17.

$$\vec{Y} = \begin{bmatrix} \beta_1 \\ \vdots \\ \beta_k \\ \vdots \\ \beta_{600} \end{bmatrix} = \begin{bmatrix} 0.335 \\ \vdots \\ 0.472 \\ \vdots \\ 0.446 \end{bmatrix} \tag{17}$$

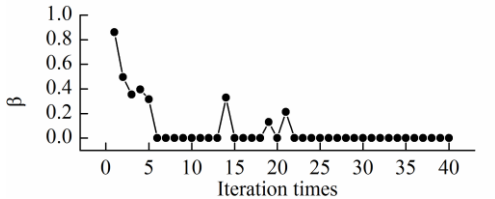

(a) Torque distribution coefficient

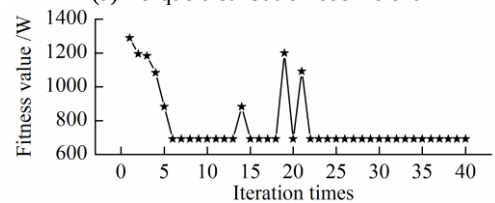

(b) Consumption fitness values

Fig. 5. Optimization results

4.6. Predictive model for torque distribution

Although Guass RBF can be used to construct complex function-relationship between the input-factor and the output-response with highly enough precision, the real-time performance of it is very difficult to be ensured. Contrarily, torque distribution model based on polynomial function has the advantage of real-time performance but with low accuracy. Furthermore, different from power loss model of motor that gives priority to model accuracy rather than real-time performance, for torque distribution model, real-time performance is necessary. Consequently, in this paper, a predictive model of torque distribution based on hybrid RBF ("polynomial + RBF") is developed, which can take the advantages of both polynomial function and RBF. According to the databases of the two-factor vehicle operation and the optimal β, under low load conditions, FRMDEV preferentially operates under single-PMSM-drive mode (β=0), and the switching boundary function between the single-PMSM-drive mode and the DMDM can be derived as:

$$T_{sw} = 65.611 - 0.137V + 0.00258V^2 + 0.0000567V^3 \tag{18}$$

Where the T_{sw} is the switching boundary between the single-PMSM-drive mode and the DMDM.

Furthermore, under the middle and high load working conditions, the FRMDEV preferentially operates

under the DMDM. To balance real-time performance and accuracy, the lower-order part of the predictive model is formed in polynomial function, and the higher-order part is in the form of Gauss RBF function, and the predictive model of torque distribution based on hybrid RBF is derived as:

$$\begin{cases} \hat{\beta} = 7.204 + \vec{A}\vec{U} + \sum_{i=1}^{m} \phi_{i\_dl} w_i + \varsigma \\ \vec{A} = \begin{bmatrix} 0.678 \\ 0.0177 \\ -1.897 \\ -1.724 \\ -1.832 \end{bmatrix}^T \quad \vec{U} = \begin{bmatrix} V \\ T_{d\_cr} \\ V^2 \\ VT_{d\_cr} \\ T_{d\_cr}{}^2 \end{bmatrix} \\ \phi_{i\_dl} = \exp\left(-\frac{\left\| \vec{x}_{dl} - \vec{C}_{i\_dl} \right\|^2}{2b_i{}^2} \right) \end{cases} \tag{19}$$

Where $\vec{x}_{dl}$ is the input vector of radial basis function defined as $[V\_dl, T_{d\_cr\_dl}]^T$, $\vec{C}_{dl}$ is the central vector of network nodes as shown in table 4.

Table 4. Key parameters of torque distribution model

Num.	w_i	RBF centers (dimensionless form)	
		V_{i_dl}	$T_{di\_cr\_dl}$
1	10.634	-0.91111	-0.75060
2	10.739	0.15556	-0.79652
3	-8.670	-0.24444	-0.12208
…	…	…	…
9	3.008	0.64444	-0.881
10	5.962	0.22222	-0.03264

4.7. Verification of model accuracy

The R^2 and RMSE of the predictive model based on hybrid RBF are confirmed as 0.992and 0.045, respectively, which means the modeling accuracy of the torque distribution model is high. Furthermore, as shown in figure 6, taking the random operation (V=24.53km.h^{-1}, T_d=99.82N.m) for example, compared with the torque distribution model based on polynomial function, the torque distribution model based on hybrid RBF can avoid the risk of forecasting failure (β>1 or β<0), and has a wider confidence interval. In general, the random sample points used for modeling hybrid RBF are almost all within the 95% confidence interval, which further verifies that the predictive torque distribution model based on hybrid RBF is with high accuracy. Moreover, as shown in figure 7, the characteristics of errors between the predictive values and the actual ones are presented, which clearly indicates the predictive accuracy of the torque distribution model based on hybrid RBF function is high.

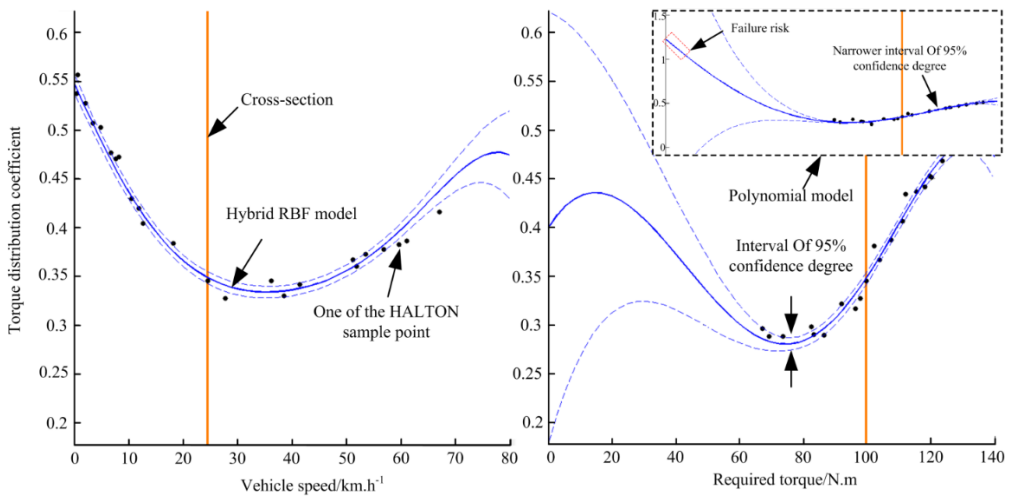

Fig. 6. Cross section of hybrid RBF torque distribution prediction model for a given point

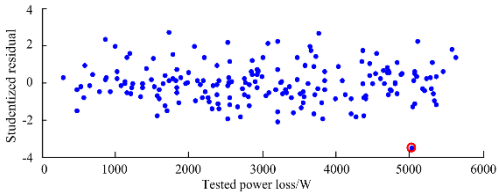

Fig. 7. Predictive accuracy of torque distribution mode

5. Verification

In order to verify the real-time performance of the torque distribution model based on hybrid RBF, the HIL system is developed as shown in figure 8. Simulink/MotoHawk is used to develop and compile the vehicle control strategy consisting of torque distribution model, braking force control module and signal transmission module et al., which are loaded into the VCU. The dynamic model of FRMDEV run in real time based on the NI real-time simulator (Real-Time Simulator, RTS), which is developed to update and send the statuses of FRMDEV.

As shown in figure 9, control strategy based on MotoHawk is designed. The time-trigger modular is designed to control the sampling step length for control strategy. Based on the system-definition modular, details about the software and hardware of the VCU are designed. The control-strategy modular is developed for the torque distribution control, attachment control and so on. Modualr 3 and 5 are designed for input and output signals control respectively.

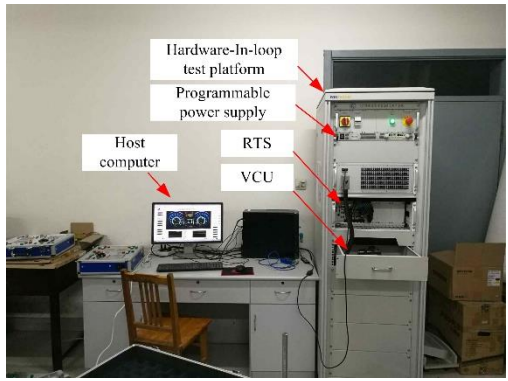

Fig. 8. HIL test of the torque distribution model

Analog and digital signals of the control strategy are presented in table 5. Taking the accelerator pedal signal 1 for example, as shown in figure 10, the voltage analog, collected by the signal acquisition pin (AN28), is transferred into the pedal degree for control strategy.

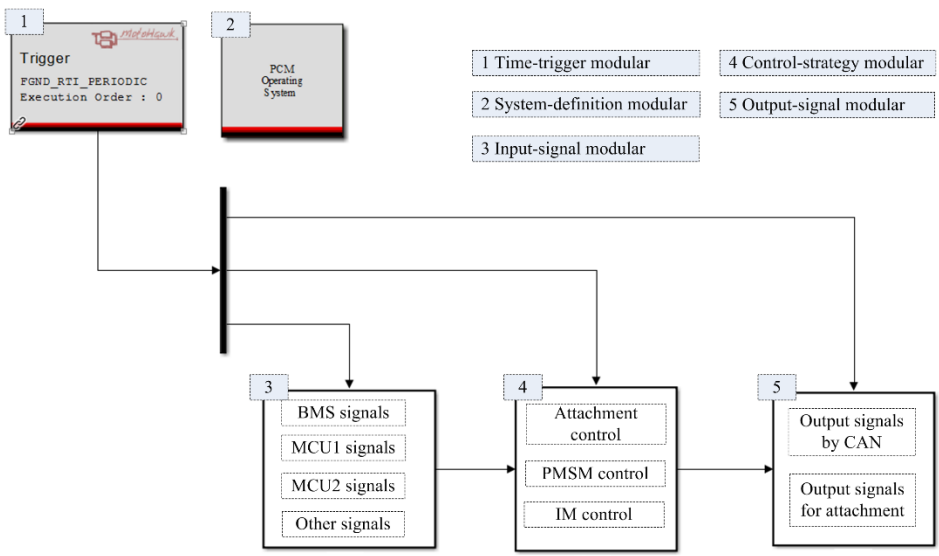

Fig. 9. Structure of vehicle control strategy based on MotoHawk

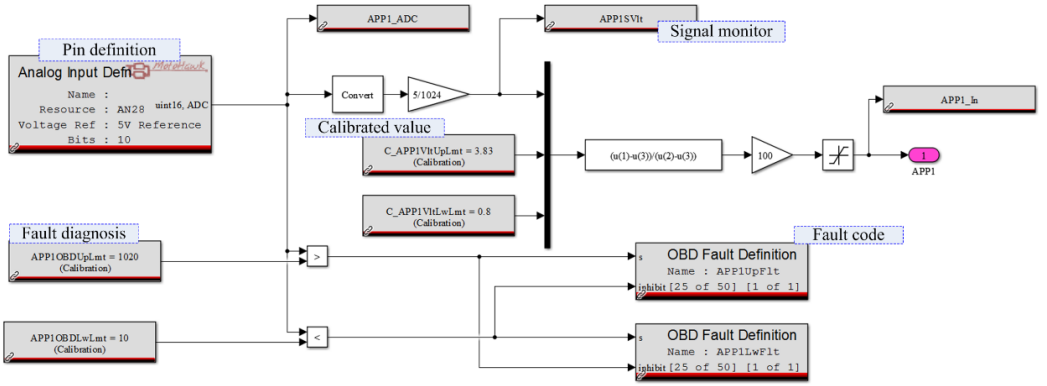

Fig.10. Analog signal processing of accelerator pedal

Table 5. Analog and digital signals of control strategy

Signals	Type	Pin	Signals	Type	Pin
Key ON	Digital	ECUP	Brake pedal	Analog	AN25
Start	Digital	AN2	P gear	Digital	AN4
VCU power	Analog	DRVP	R gear	Digital	AN15
Sensor power	Analog	XDRP	D gear	Digital	AN23
Accelerator pedal 1	Analog	AN28	Pressure of vacuum pump	Analog	AN3
Accelerator pedal 2	Analog	AN30	Pressure ground	GND	XDRG1
Pedal ground 1	GND	XDRG1	Coolant	Analog	AN9
Pedal ground 2	GND	XDRG2	Coolant ground	GND	XDRG2

As shown in figure 11(a) and 11(b), the results of the torque distribution model under typical urban working conditions are obtained with the use of HIL test. The test results show that, the predictive model of torque distribution based on hybrid RBF shows perfect real-time performance, which means that with the use of hybrid RBF method, the predictive torque distribution model is able to meet the real-time requirement of engineering application.

Furthermore, compared with the original FRMDEV with torque distribution strategy based on rule algorithm (Sun Binbin, et al., 2017), the predictive model of torque distribution based on hybrid RBF can improve the drive efficiency significantly. Specially, compared with the original scheme, the new one can reduce driving energy consumption by 9.51% under urban drive cycle, as shown in figure 11(c).

6. Conclusions

In order achieve high-efficiency drive of FRMDEV, a predictive model of torque distribution based on hybrid RBF is proposed in this paper, and HIL test is carried out. Owing to HALTON sequence method, fewer test cost can be achieved for modeling motor power loss. Gauss RBF is an effective method to establish the response surface model of motor power loss with high precision. The mathematical method of hybrid RBF can be used to develop torque distribution model with prefect real-time performance, high accuracy and optimal drive efficiency. Compared with the original torque distribution based on rule algorithm, the new predictive torque distribution based on hybrid RBF can reduce driving energy consumption by 9.51% under urban cycle.

Acknowledgement

This work was supported by the National Natural Science Foundation Project of China (51805301), the Natural Science Foundation Project of Shandong (ZR2019BEE043 and ZR2018LF009), the Scientific Research Project of Universities in Shandong (J18KA021), and the Zibo City-Shandong University of Technology Cooperative Projects (2017ZBXC165).

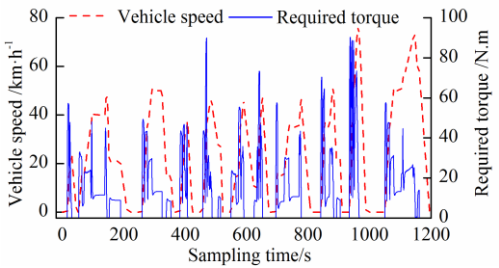

(a) Vehicle speed and required torque

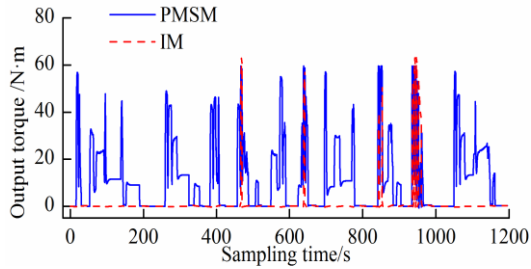

(b) Torque distribution based on Hybrid RBF model

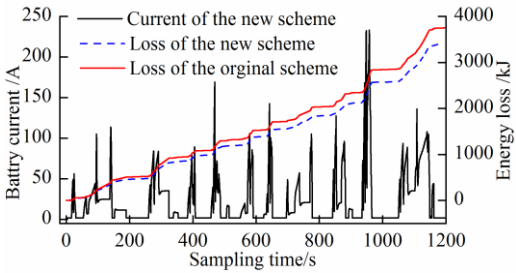

(c) Current and energy consumption

Fig. 11. Tested results of torque distribution based on hybrid RBF

References

[1] BHATTI, A. R., SALAM, Z., 2018. A rule-based energy management scheme for uninterrupted electric vehicles charging at constant price using photovoltaic-grid system *Renewable Energy*, 125, 384-400.

[2] SUN, B., GAO, S., MA, C., 2016. Mathematical Methods Applied to Economy Optimization of an Electric Vehicle with Distributed Power Train System. *Mathematical Problems in Engineering*, 2016, 4949561.

[3] SUN, B., ZHANG, T., GAO, S., GE, W., LI, B., 2018. Design of brake force distribution model for front-and-rear-motor-drive electric vehicle based on radial basis function. *Archives of Transport*, 48(4), 87-98

[4] CHINA AUTOMOTIVE TECHNOLOGY RESEARCH CENTER, NISSAN (CHINA) INVESTMENT CO., LTD., DONGFENG MOTOR COMPANY, 2015. *Report on development of new energy automotive industry*. Beijing: Social Sciences Literature Press.

[5] GUO, H., HE, H., XIAO, X., 2014. A Predictive Distribution Model for Cooperative Braking System of an Electric Vehicle. *Mathematical Problems in Engineering*, 2014, 1-11.

[6] PENG, J., HE, H., XIONG, R., 2017. Rule based energy management strategy for a series–parallel plug-in hybrid electric bus optimized by dynamic programming. *Applied Energy*, 185(2), 1633-1643.

[7] KUMAR, M. S., REVANKAR, S. T., 2017. Development scheme and key technology of an electric vehicle: An overview. *Renewable and Sustainable Energy Reviews*, 2017, 1266-1285.

[8] MERKISZ-GURANOWSKA, A., PIELECHA, J., 2014. Passenger cars and heavy duty vehicles exhaust emissions under real driving conditions. *Archives of Transport*, 31(3), 47-59.

[9] SULAIMAN, N., HANNAN, M. A., MOHAMED, A., KER, P. J., MAJLAN, E. H., & DAUD, W. W., 2018. Optimization of energy management system for fuel-cell hybrid electric vehicles: issues and recommendations. Applied energy, 228, 2061-2079.

[10] MUTOH, N., 2012. Driving and Braking Torque Distribution Methods for Front-and Rear-Wheel-Independent Drive-Type Electric Vehicles on Roads With Low Friction Coefficient. *IEEE Transactions on Industrial Electronics*, 59(7), 3919-3933.

[11] ADDERLY, S. A., MANUKIAN, D., SULLIVAN, T. D., & SON, M., 2018. Electric vehicles and natural disaster policy implications. *Energy Policy*, 2018:437-448.

[12] SUN, B., GAO, S., WANG P., ET AL., 2017. A Research on Torque Distribution Strategy for Dual-Motor Four-Wheel-Drive Electric Vehicle Based on Motor Loss Mechanism. *Automotive engineering*, 39(4), 386-393.

[13] SUN, D., LAN, F.,, HE, X., 2016. Study on Adaptive Acceleration Slip Regulation for Dual-motor Four-wheel Drive Electric Vehicle. *Automotive engineering*, 38(5), 600-619.

[14] SUN, B., GAO, S., WU Z., ET AL., 2017. Parameters Design and Economy Study of an Electric Vehicle with Powertrain Systems in Front and Rear Axle. *International Journal of Engineering Transactions A: Basics*, 29(4), 454-463.

[15] CHEN, S. Y., WU, C. H., HUNG, Y. H., & CHUNG, C. T., 2018. Optimal strategies of energy management integrated with transmission control for a hybrid electric vehicle using dynamic particle swarm optimization. *Energy*, 160, 154-170.

[16] SHI,Y., 2014. *Research on energy management strategy of tandem hybrid hydraulic vehicle based on fuzzy logic*, Master of Engineering, Jilin University, China.

[17] XI, Z., 2013. *Vehicle energy management: modeling, control and optimization*. Beijing: China Machine Press.